Platinum and Palladium Films Obtained by Low-Temperature MOCVD for the Formation of Small Particles on Divided Supports as Catalytic Materials

Jean-Cyrille Hierso,[†] Roselyne Feurer,[‡] and Philippe Kalck*,[†]

Laboratoire de Catalyse, Chimie Fine et Polymères and the Laboratoire des Interfaces et Matériaux (UPRESA-CNRS 5071), Ecole Nationale Supérieure de Chimie de Toulouse, 118 route de Narbonne, 31077 Toulouse Cedex 4, France

Received June 30, 1999. Revised Manuscript Received October 29, 1999

CVD studies devoted to platinum and palladium deposition on planar substrates for microelectronics have clearly shown that it is possible to reach high-quality deposits at temperatures above 200 °C. Attempts to prepare pure metallic deposits at temperatures around 100 °C and even lower are of general interest, since a number of temperature-sensitive supports could be then exploited. An other attracting issue in the field of catalysts elaboration is presented here. $Pt(hfa)_2$, $PtMe_2(cod)$, $Pd(Cp)(\eta^3\text{-}C_3H_5)$, and $Pd(\eta^3\text{-}C_3H_5)(hfa)$ have been selected to produce by MOCVD platinum and palladium deposits on planar and on divided supports. The EI-mass spectrometry of the precursor complexes as well as their thermal behavior are reported (TGA, DSC, vapor pressure equations). Introduction of hydrogen in the carrier gas results in a dramatic decrease of the deposition temperature (35−120 °C) of the complexes. XPS and electron microprobe analyses have shown that $PtMe_2(cod)$, $Pd(Cp)(\eta^3\text{-}C_3H_5)$, and $Pd(\eta^3\text{-}C_3H_5)(hfa)$ are suitable precursors to produce pure thin films at these remarkably low temperatures. $Pt(hfa)_2$ gave poor results since the deposits are contaminated with fluorine, oxygen, and principally carbon. Using the CVD method in a fluidized bed under reduced pressure conditions allowed the deposition of the metals on porous divided substrates. Highly dispersed metallic particles of palladium and platinum on silica can be prepared under very mild temperatures (below 120 °C). TEM micrographies revealed a narrow size dispersion of the nanoparticles (average size 1−3 nm). EDX analyses did not show any contamination of the deposits. A high supersaturation regime was identified to be a crucial parameter in the fluidized bed-MOCVD method, allowing a good nucleation rate with regard to the growth rate. Catalysts prepared by this method, and containing palladium and platinum on porous silica, were highly active for the dehydrogenation of cyclohexane.

Introduction

In heterogeneous catalysis, the preparation of the catalyst is crucial to its subsequent performance. Mostly, the active catalytic species consists of highly dispersed pure metal particles supported on the surface of a porous material. Among the methods of preparation which have been described, metal−organic chemical vapor deposition (MOCVD) has received only limited attention.[1] The chemical vapor deposition method,[2] as distinct from the impregnation of a solid from the vapor phase,[3] allows the direct deposition of the active species on the support without any further treatment. This eliminates the traditional steps of impregnation, washing, drying, calcination, and reduction.[1] Most of the drawbacks of classical methods of catalyst preparation due to liquid solvents are avoided: the redistribution of active sites during drying, surface poisoning during impregnation and the migration of particles during sintering in the steps of preparation involving high temperatures. Moreover, the structure of the support, in particular its porosity and its specific area, are unaltered by MOCVD. Our laboratories have reported a method for the preparation of catalysts which provides a homogeneous dispersion of metal particles on a divided support by MOCVD in a fluidized bed reactor (FB-MOCVD).[4−6]

In the course of CVD studies devoted to palladium deposition on planar substrates for microelectronics, $Pd(Cp)(\eta^3\text{-}C_3H_5)$ and $Pd(\eta^3\text{-}C_3H_5)(hfa)$, where hfa is the ligand hexafluororacetylacetonato, were shown by Girolami et al.[7] and by Puddephatt et al.[8] respectively

[†] Laboratoire de Catalyse, Chimie Fine et Polymères.
[‡] Laboratoire des Interfaces et Matériaux (UPRESA-CNRS 5071).

(1) Schwarz, J. A.; Contescu, C.; Contescu, A. *Chem. Rev.* **1995**, *95*, 477.
(2) (a) Zinn, A.; Niemer, B.; Kaesz, H. D. *Adv. Mater.* **1992**, *5*, 375. (b) Hampden-Smith, M. J., Kodas, T. T., Eds. *The Chemistry of Metal CVD*; VCH: New York, 1994.
(3) (a) Dossi, C.; Bartsch, A.; Losi, P. *Adv. Synth. Methodol. Inorg. Chem.* **1991**, 83. (b) Sordelli, L.; Martra, G.; Psaro, R.; Dossi, C.; Coluccia, S. *J. Chem. Soc., Dalton Trans.* **1996**, 720.
(4) Serp, P.; Feurer, R.; Morancho, R.; Kalck, P. *J. Mol. Catal.* **1995**, *101*, 107.
(5) Serp, P.; Feurer, R.; Morancho, R.; Kalck, P. *J. Catal.* **1995**, *157*, 294.
(6) Hierso J.-C.; Serp, P.; Feurer, R.; Kalck, P. *Appl. Organomet. Chem.* **1998**, *12*, 161.

10.1021/cm990406e CCC: $19.00
Published on Web 01/12/2000

to lead to excellent deposits. Pd(η^3-C_3H_5)(hfa) gave pure palladium metal in the presence of oxygen at temperatures above 330 °C and Pd(Cp)(η^3-C_3H_5) at 250 °C without reactive gas. Concerning platinum, Kaesz et al. discovered that pure platinum was obtained using Pt(Me)$_3$(Cp) in the presence of hydrogen at temperatures around 200 °C.[9] These examples clearly show that at the present time, it is possible to reach high-quality deposits of platinum and palladium at temperatures above 200 °C. However, for several applications, particularly when the support is very temperature-sensitive,[10] these temperatures of decomposition appear to be still too high, so that studies to prepare pure metallic deposits at temperatures around 100 °C and even lower are of great general interest.[11]

The present work concerns the preparation of homogeneous dispersions of pure palladium and platinum particles on powdered silica, by FB-MOCVD under very mild conditions. MOCVD on both planar substrates and divided porous materials was carried out to compare and possibly to correlate the results obtained. We have examined the physicochemical properties of several volatile palladium and platinum compounds and determined ideal conditions for their use by MOCVD on planar supports in a classical hot wall reactor. We have also managed to identify which fundamental parameters and/or reaction steps are retained during the switch from a planar support to a divided support, and which are modified. This information has allowed us to prepare dispersions of nanoparticles on divided supports, which are catalytically active in hydrogenation and dehydrogenation reactions. Crucially, the size and dispersion of the nanoparticles is not affected after many catalytic runs at 500 °C. Finally, the present work shows that the careful CVD study targeted at the crucial parameters, like high supersaturated vapor pressure, allows a great part of the results on porous supports to be predicted: it was thus demonstrated, that Pd(η^3-C_3H_5)(hfa), Pd(Cp)(η^3-C_3H_5), and PtMe$_2$(cod) are suitable precursors to obtain pure metallic films as well as active metallic particles by CVD below 100 °C.

Results and Discussion

MOCVD of Palladium Films from Pd(η^3-C_3H_5)(hfa) and Pd(Cp)(η^3-C_3H_5). We have previously reported our results concerning the low-temperature deposition of palladium films on planar supports using Pd(η^3-C_3H_5)(hfa) and Pd(Cp)(η^3-C_3H_5) as precursors.[12] Pure crystalline deposits can be obtained at temperatures as low as 30−60 °C in the presence of hydrogen (total pressure 50 Torr), with carbon contamination less than 1 atom % in the case of Pd(η^3-C_3H_5)(hfa). The deposits were obtained with a high growth rate due to the high volatility of these two precursors: the vapor pressures at 100 °C are 2.5 Torr for Pd(η^3-C_3H_5)(hfa) and 25 Torr for Pd(Cp)(η^3-C_3H_5).

Table 1. Electron Impact (70 keV) Mass Spectrum of Pt(hfa)$_2$

m/q	intensity (%)	fragments
609	75	$[Pt(hfa)_2]^+$
590	16	$[(hfa)Pt-C_5HO_2F_5]^+$
540	4	$[(hfa)Pt-C_4HO_2F_3]^+$
512	8	$[CF_3CHCOPt(hfa)]^+$
430	25	$[CO-Pt(hfa)]^+$
402	3	$[Pt(hfa)]^+$
333	6	$[Pt-C_4HO_2F_3]^+$
291	8	$[Pt-O-C_2F_3]^+$
276	8	$[C_2OPt-O-C_2H]^+$
236	8	$[Pt-O-C_2H]^+$
223	5	$[CO-Pt]^+$
91	95	$[COCHCF_2]^+$
69	100	$[CF_3]^+$

Table 2. EI-Mass Spectrum of PtMe$_2$(cod) at 70 keV

m/q	intensity (%)	fragments
333	13	$[PtMe_2(cod)]^+$
317	37.5	$[PtMe(cod)]^+$
302	23	$[Pt(cod)]^+$
273	10	$[Pt(C{=}CC_2H_4CH{=}C)]^+$
260	3	$[PtCC_2H_4CH{=}C]^+$
247	5	$[Pt(CHCH_2CH{=}CH)]^+$
233	3.5	$[PtCHCH{=}CH]^+$
221	7	$[C-PtMe]^+$
209	8	$[PtMe]^+$
149	13	recombination (cod+fragments)
105	13	$[CCH_2C_2H_2C_2H_4CH{=}C]^+$
91	26	$[CC_2H_2C_2H_4CH{=}C]^+$
77	52	$[C{=}CC_2H_4CH{=}C]^+$
67	27	$[CHC_2H_4CH{=}CH]^+$
53	37.5	$[CHCH_2CH{=}CH]^+$
41	87.5	$[CH_2CH_2CH]^+$
39	100	$[CHCH{=}CH]^+$

Suitability of Pt(hfa)$_2$ and PtMe$_2$(cod) as MOCVD Precursors. Several groups have examined the MOCVD of platinum films with a view to microelectronic applications. Kaesz et al. reported that pure platinum was obtained using PtCpMe$_3$ in the presence of hydrogen;[9,13] unfortunately, the yield of this precursor was only 52%.[14] Dryden and co-workers have shown that PtMe$_2$(cod), prepared in 82% yield,[15] was a suitable precursor to pure platinum deposits (although still containing 4% C and 2% O) at 200−250 °C in the presence of hydrogen. The complex Pt(hfa)$_2$ (hfa = hexafluoroacetylacetonato ligand) has been extensively studied by van den Berg et al. in deposition by laser photolysis with the view to elaborate microelectronic or optoelectronic devices,[16] and by Wolfrum et al. to produce catalytic metal powders.[17]

We chose to examine the properties of PtMe$_2$(cod) and Pt(hfa)$_2$ as possible precursors for FB-MOCVD. These compounds appeared promising because of their good volatility, ease of preparation in high yield and adequate air- and moisture-stability.[18]

(7) Gozum, J. E.; Pollina, D. M.; Jensen, J. A.; Girolami, G. S. *J. Am. Chem. Soc.* **1988**, *110*, 2688.
(8) (a) Yuan, Z.; Puddephatt, R. J. *Adv. Mater.* **1994**, *6*, 51. (b) Zhang, Y.; Choi, S. W.-K.; Puddephatt, R. J. *J. Am. Chem. Soc.* **1997**, *119*, 9295 and references therein.
(9) Xue, Z.; Strouse, M. J.; Shuh, D. K.; Knobler, C. B.; Kaesz, H. D.; Hicks R. F.; Williams, R. S. *J. Am. Chem. Soc.* **1989**, *111*, 8779.
(10) Duan, Z.; Hampden-Smith, M. J. *Chem. Mater.* **1993**, *5*, 994.
(11) Maury, F. *Chem. Vap. Deposition* **1996**, *2*, 113 and references therein.
(12) Hierso, J.-C.; Satto, C.; Feurer, R.; Kalck, P. *Chem. Mater.* **1996**, *8*, 2481.
(13) Xue, Z.; Thridandam, H.; Kaesz, H. D.; Hicks R. F. *Chem. Mater.* **1992**, *4*, 162.
(14) Chen, Y. J.; Kaesz, H. D.; Thrindandam, H.; Hicks, R. F. *Appl. Phys. Lett.* **1988**, *53*, 1591.
(15) Dryden, N. H.; Kumar, R.; Ou, E.; Rashidi, M.; Roy, S.; Norton, P. R.; Puddephatt, R. J.; Scott, J. D. *Chem. Mater.* **1991**, *3*, 677.
(16) Lecohier, B.; Philippoz, J. M.; van der Berg, H. *J. Vac. Sci. Technol. B* **1992**, *10*, 262 and references therein.
(17) Willwohl, H.; Wolfrum, J.; Zumbach, V. *J. Phys. Chem.* **1994**, *98*, 2242.
(18) Hierso, J.-C.; Feurer, R.; Kalck, P. *Coord. Chem. Rev.* **1998**, *178−180*, 181.

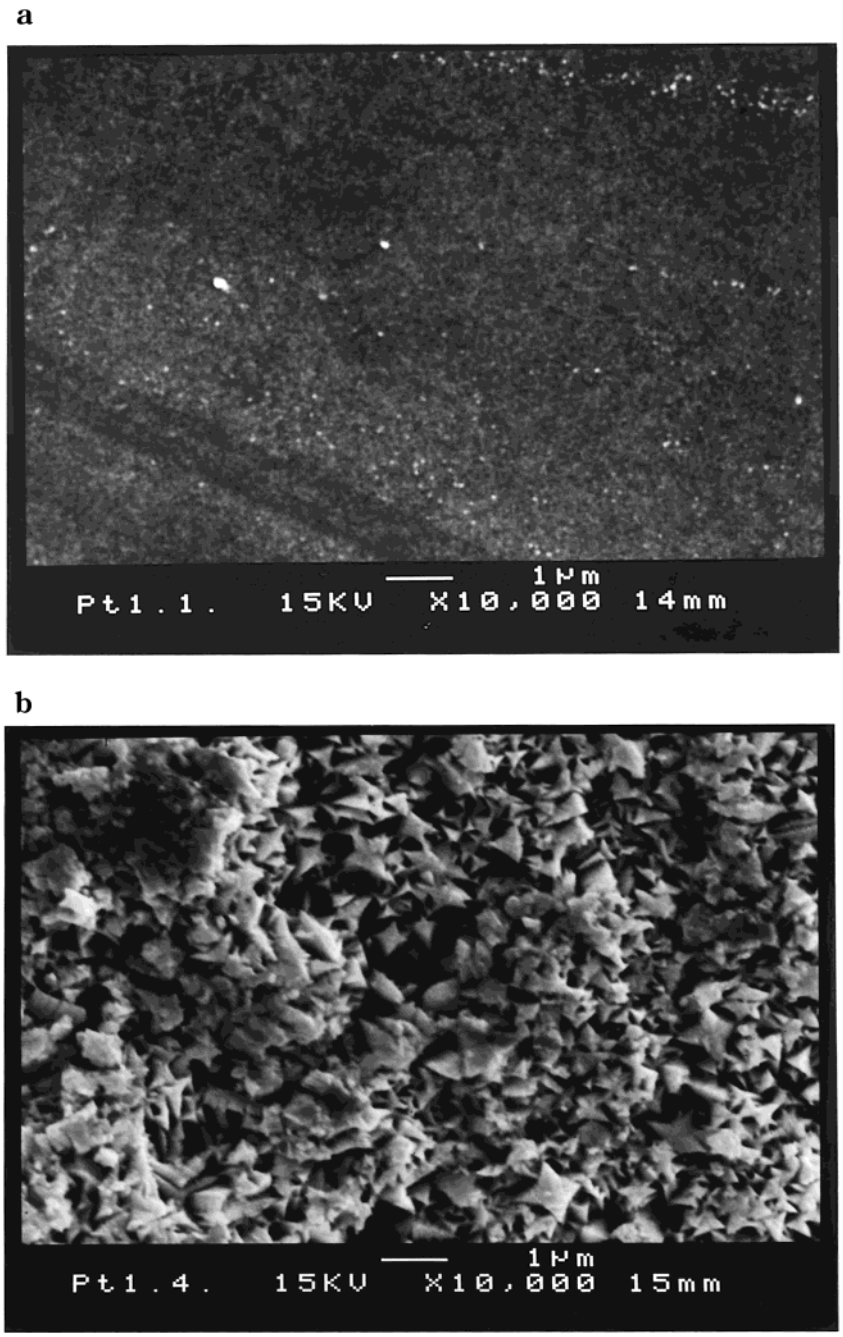

Figure 1. Scanning electron microscope (SEM) photographs of the platinum thin films produced from $Pt(hfa)_2$: (a) films deposited at 400 °C in the absence of H_2 and (b) films deposited at 140 °C in the presence of H_2.

EI-MS of Pt(hfa)$_2$. Electron impact mass spectrometry is a useful tool for probing the decomposition pathways that a compound might follow during its thermolysis, even if it is necessary to be careful of direct conclusions. Indeed, the electronic bombardment allows the estimation of the relative strength of some internal chemical bonds of the studied molecule through it characteristic fragmentation pattern. In particular, the observation of naked metal cations in the EI mass spectrum is an indication that it is possible to completely remove the ligands as required during MOCVD to produce pure metal deposits.

The EI mass spectrum of $Pt(hfa)_2$ (see Table 1) indicated a considerable thermal stability. The parent molecular ion (m/q = 609) was detected with a high intensity. Signals at m/q = 590 and m/q = 540, resulting from the loss of a fluorine atom and a CF_3 group respectively, can also be observed. The observation of a fragment at m/q = 430, assigned to $[(CO)Pt(hfa)]^+$, is consistent with a strong platinum−oxygen bond. Hence, the internal ligand bonds appear to be cleaved more easy than the platinum−ligand bonds: significantly, no signal for $[Pt]^+$ was observed.

EI-MS of PtMe$_2$(cod). The platinum−ligand bonds in $PtMe_2(cod)$ appeared to be less stable under EI-MS conditions than in $Pt(hfa)_2$ (see Table 2). Although we were still unable to observe a signal corresponding to $[Pt]^+$, the ions $[PtMe(cod)]^+$ (m/q = 317, r.i. = 37.5%) and $[Pt(cod)]^+$ (m/q = 302, r.i. = 23%) could be clearly detected. The cyclooctadiene ligand could also be cleanly removed, as evidenced by the signal at m/q = 209 (r.i. = 8%) assigned to $[PtMe]^+$. However, there were also

several peaks arising from the fragmentation of the cyclooctadiene ligand with retention of a portion bound to platinum.

Thermal Behavior of $Pt(hfa)_2$ and $PtMe_2(cod)$. The thermal behavior of the complexes was probed directly by thermogravimetric analysis (TGA) and differential scanning calorimetry (DSC). The DSC trace for $Pt(hfa)_2$ under helium (1 atm) shows a sharp peak at 150 °C corresponding to the endothermic melting of the complex ($\Delta H = +122.9$ J g^{-1}), while a broad disymmetric peak at 200 °C is consistent with its endothermic vaporization ($\Delta H = +217.3$ J g^{-1}). TGA experiments showed that a continuous weight loss occurred during vaporization which was greater than 92%. Almost all the complex was vaporized at 220 °C, and coupled mass spectrometry measurements revealed the presence of $Pt(hfa)_2$ in the vapor phase. Hence, the decomposition of $Pt(hfa)_2$ does not occur significantly under these conditions. Moreover, our DSC and TGA results for $PtMe_2(cod)$ are entirely consistent with those reported by Dryden et al.[15]

Control of a given CVD process entails knowledge of the partial pressure of the precursors under the experimental conditions. The temperature dependence of the vapor pressure for the two complexes follows the Clausius−Clapeyron equations given below (for pressures in Torr).

$$Pt(hfa)_2: \ln p = -9320/T + 29.3$$

$$PtMe_2(cod): \ln p = -5441/T + 17.2$$

The heats of sublimation obtained from these equations are 77 ± 4 kJ mol^{-1} for $Pt(hfa)_2$ and 45 ± 2 kJ mol^{-1} for $PtMe_2(cod)$. The vapor pressures of the complexes at 100 °C are 0.5 and 0.1 Torr, respectively.

Elaboration and Characterization of Platinum Thin Films. *Use of $Pt(hfa)_2$ as Precursor.* MOCVD experiments were initially carried out in a classical hot wall reactor on glass planar supports. Under a helium pressure of 50 Torr, the decomposition of $Pt(hfa)_2$ was observed above 400 °C, yielding bright metallic and adherent films. However, decomposition was only partial, and about 75% of the complex were recovered under a solid form beyond the deposit area, regardless of the contact duration. The introduction of 3−12% hydrogen resulted in a minimum deposition temperature of 140 °C. The films obtained were black and less adherent than in the previous case. Attempts to reach better conditions of elaboration at lower temperatures or higher partial pressures of hydrogen were unsuccessful. Although the carrier gas flow and the partial pressure of hydrogen were varied across a wide range, the proportion of the complex decomposed to form the film did not exceed 25%. The deposits were roughly similar on varying the decomposition temperature between 140 °C and 200 °C.

Scanning electron micrographs of the two films are shown in Figure 1. Films deposited at 400 °C in the absence of hydrogen are smooth on the micrometer scale (Figure 1a), showing a grain size of about 100 nm and an isotropic growth. Films deposited at 140 °C in the presence of hydrogen display pyramids of about 1 μm high (see Figure 1b), characteristic of an anisotropic growth in the ⟨111⟩ direction. This was confirmed by

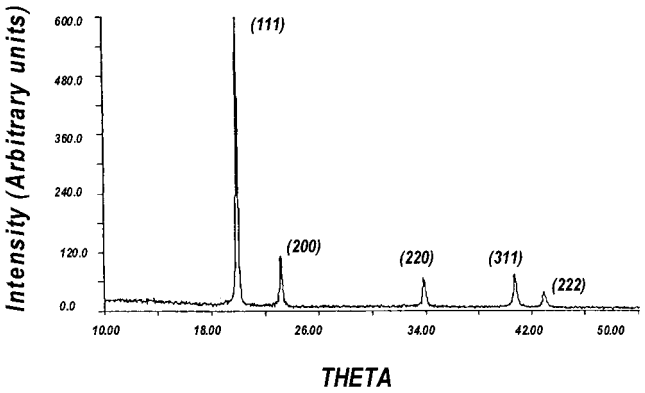

Figure 2. X-ray diffraction pattern of a Pt film from $Pt(hfa)_2$ at 140 °C in the presence of H_2.

X-ray diffraction pattern (see Figure 2), in which the overintensity of the (111) peak is easy to observe.

Analysis of the films by XPS revealed, in addition to the expected signals due to platinum, peaks due to carbon (1s) and oxygen (Auger peak). Films deposited at 400 °C in the absence of hydrogen were also contaminated with fluorine. Etching the surface with Ar^+ for 15 min removed the oxygen and diminished the signal due to carbon, but the signal due to fluorine from the films deposited at high temperatures was unchanged. Semiquantitative analyses have shown that in any case, even after etching, the amounts of carbon incorporation are around 8 wt % (45 atom %). Electron microprobe experiments on deposits, obtained at 140−200 °C in the presence of hydrogen, confirmed the presence of platinum, carbon, and oxygen, fluorine being not detected. Analyses on various areas revealed great inhomogeneities in the deposits with high levels of carbon contamination which can reach 10 wt % (or 65 atom %) with oxygen incorporation of up to 1 wt % (6 atom %).

Use of $PtMe_2(cod)$ as Precursor. $PtMe_2(cod)$ decomposed above 240 °C under a helium pressure of 50 Torr to give gray metallic films. Addition of hydrogen to the gas flow reduced dramatically the decomposition temperature to 90 °C and gray adhesive metallic films were also obtained. From these general observations the experimental conditions were optimized with the objective to reduce the temperature of deposition and to produce deposits with high purity. The coatings were realized at pressures ranging between 30 and 100 Torr to vary the molar ratio of the complex in the gas phase. The optimum conditions for deposition were a temperature of 100−120 °C, a total pressure of 30−60 Torr, and a hydrogen content in the helium carrier of 3−6% v/v. Unlike the case of $Pt(hfa)_2$, total decomposition of $PtMe_2(cod)$ was achieved under these conditions.

The platinum deposits obtained in the presence or in the absence of hydrogen present in SEM observations large grains whose sizes range between 0.2 and 1 μm. By using EDX-coupled analysis, the presence of platinum was evidenced by the Mα1 peak at 2.05 keV. X-ray spectra have shown that no particular orientation was adopted by metallic platinum during the growth of the films. XPS spectra are shown on Figure 3 for a deposit obtained at 110 °C and 60 Torr and with 3% of H_2/He. All the peaks due to metallic platinum were assigned. Semiquantitative analyses revealed the presence of

Table 3. Conditions of Deposition of Palladium and Platinum by MOCVD

precursor	sublimation T (°C)	deposition T (°C)	He gas flow (mL min^{-1})	H_2 gas flow (mLmin^{-1})/ % of total flow	total P (Torr)	precursor molar ratio
Pd(Cp)(η^3-C_3H_5)	50	45−60	86	0.8/1%	50−60	1.0×10^{-2}
Pd(η^3-C_3H_5)(hfa)	50	35−60	86	0.8/1%	50−60	2.4×10^{-3}
Pt(hfa)$_2$	55−75	140−150	43	2.6/6%	45−60	3.0×10^{-4} to 2.2×10^{-3}
PtMe$_2$(cod)	70−80	90−120	86	2.6/3%	30−60	4.8×10^{-4} to 1.5×10^{-3}

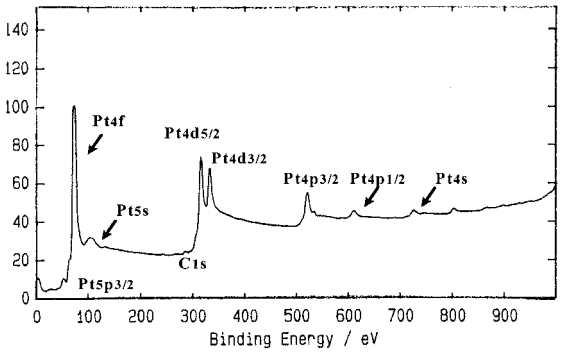

Figure 3. XPS spectra of a platinum deposit obtained at 110 °C under 3% of H_2 from PtMe$_2$(cod).

small amounts of carbon, i.e., 1.4 wt % (or 15 atom %), and no other heteroelement was detected. For the deposits performed at 240−280 °C in the absence of hydrogen, higher levels of carbon contamination were noted. Electron microprobe analyses confirmed the XPS results since for the deposits obtained at 100 °C in the presence of H_2 a 1.3 wt % contamination in carbon was measured. The results were identical in the various areas on the samples.

CVD of Platinum and Palladium on Porous Divided Substrate. The experiments have been carried out in an especially designed low-pressure fluidized bed reactor which has been described elsewhere.[12] A silica with a 170 m^2 g^{-1} specific area was used for all the experiments presented here. After selection of good conditions of temperature, pressure, and amounts of hydrogen for the deposition of palladium and platinum on flat glass surfaces (see Table 3), we then transferred these experimental conditions to the regime of FB-MOCVD to deposit the metals on porous silica powder. To keep the temperature of deposition as low as possible, and hence to avoid the migration and coalescence of the metal particles produced, hydrogen was introduced into the carrier gas stream just before it reached the fluidized bed. The durations of the experiments were determined by the desired loading of the support, assuming complete decomposition of the precursor. All the resulting powders have been characterized by elemental analysis (palladium and platinum), TEM coupled with EDX, and specific area determinations.

Palladium Deposits on Silica Powder. The use of Pd(Cp)(η^3-C_3H_5) as a FB-MOCVD precursor allows the deposition of 0.72 wt % palladium on powdered silica in 20 min at 60 °C. Transmission electron microscopy (see Figure 4b) shows a high and even dispersion of the palladium aggregates, which are homogeneous in size with a mean diameter of 2.0 ± 0.5 nm. These observations are confirmed by the histogram of particles size, resulting from the treatment of various micrographies. Moreover, as shown in Table 4, the initial specific area remains unchanged after the experiment. A higher loading of palladium (2.8 wt %, Figure 4c) is possible by increasing the deposition time, but this leads to a slight increase in the size of the aggregates (see Table 4). At a loading of 4.04 wt %, several large aggregates greater than 10 nm diameter were observed (Figure 4d). BET surface area measurements showed only a slight decrease in the specific area of the silica after deposition of the palladium. For all these deposits, EDX spectroscopy failed to detect any heteroatom contamination, as it was previously observed for deposits on planar supports under the same conditions.

Similar results were obtained using Pd(η^3-C_3H_5)(hfa) as the precursor, although the deposition is slightly slower (due to the lower vapor pressure of precursor in the experiment) with, for instance, 0.35 wt % loading being achieved in 30 min at 45 °C. Finally, from this complex, according to the amount of metal deposited (and to the deposition duration time) the particles sizes varies between 1 and 5 nm for loading ranging from 0.35 wt % to 4 wt % of palladium.

Platinum Deposits on Silica Powder. The complex Pt(hfa)$_2$ was used at 140 °C in the presence of 3−6% of hydrogen in the carrier gas. As expected from our results on planar supports, Pt(hfa)$_2$ proved disappointing as a precursor for FB-MOCVD. An adsorption−reduction process is apparent, with the silica grains becoming first orange-yellow before turning gray. Decomposition of the complex is always incomplete, even when using higher temperatures, higher concentrations of hydrogen and longer deposition times. The deposition of platinum is not homogeneous over the whole bed of silica grains and different samples of silica from the same deposition batch gave platinum contents ranging between 1.7 wt % and 5.7 wt %. TEM examination of the deposits (Figure 5a) indicated a great heterogeneity in particle size, with aggregates larger than 100 nm being found close to those of less than 10 nm in diameter. Unlike the case of the palladium precursors, EDX measurements indicated severe contamination by light elements, particularly carbon.

PtMe$_2$(cod) was much more satisfactory as a precursor for FB-MOCVD. This complex gave particularly nice results since, using the conditions determined in the films studies (see Table 3), the size and the repartition of the particles are remarkably homogeneous below a 4 wt % metal loading. As previously observed for deposits on planar substrates starting from this precursor, only platinum was detected from EDX analyses. The BET specific area was not modified by the deposition. After an experiment of 1 h the support was charged with 1.02 wt % of platinum, the size of the particles being below 1 nm. For duration of 2 and 3 h the charge of platinum increases regularly (2.3 wt % and 3.8 wt % respectively), whereas in both cases the size of the particles remains stable around 3 nm. The micrographs on Figure 5b−d show the quality of the deposits, and particularly their large dispersion. The histograms on Figure 6 represent

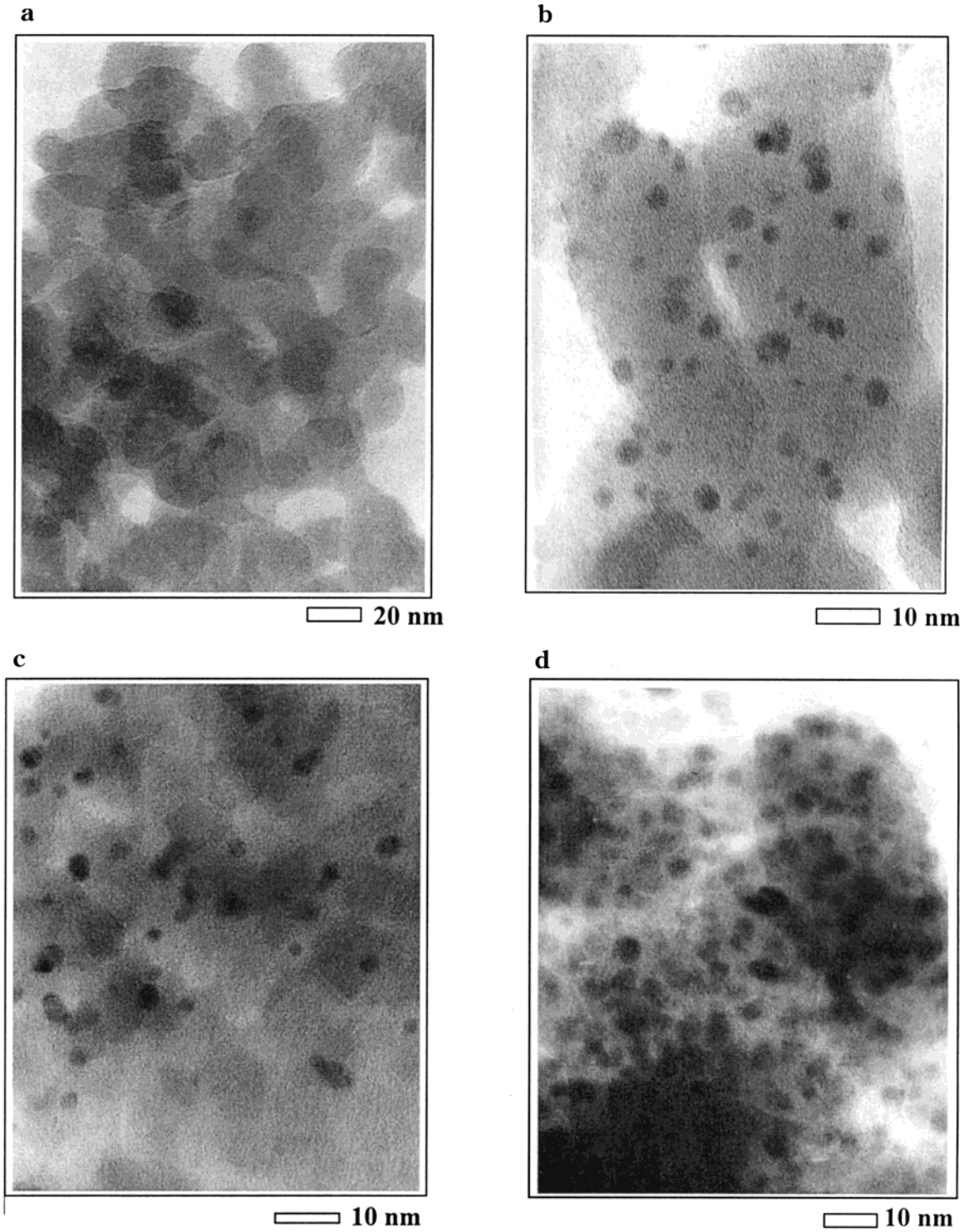

Figure 4. Transmission electron microscopy (TEM) photographs of palladium deposits supported on silica: (a) pure silica, (b) Pd/SiO_2 0.72 wt %, (c) Pd/SiO_2 2.48 wt %, and (d) Pd/SiO_2 4.04 wt %.

the various sizes of particles from Figure 5; they display a very narrow size distribution whatever the loading of metal.

Fundamental Remarks and Discussion Concerning MOCVD on Divided Supports. Although the mechanisms of CVD on planar substrates have been widely investigated, very few studies have addressed the problem of CVD of noble metals on porous powder supports. With the view to correlate the two approaches, several questions should be addressed: particularly, what is the deciding step which should drive the CVD process in the conditions we used, then what are the essential differences and similarities between a deposition on a planar support and a deposition on a porous divided support, and finally what fundamental parameters will permit to favor the formation of small and dispersed metallic particles?

The classical model of CVD recognizes three successive main steps: gas-phase reactions, adsorption of the precursor, and its subsequent decomposition. As shown previously for CVD from palladium complexes,[12] the contribution of the gas-phase reactions under low pres-

Table 4. Characteristics of the Deposits after Fluidized Bed-MOCVD Experiments

precursors	figure	metal loading (%)	av particle size (nm)	EDX analyses	BET surface ($m^2\ g^{-1}$)
Pure silica	4a			Si, O	170
Pd(Cp)(η^3-C_3H_5)	4b	0.72	2.0 ± 0.5	Pd	169
Pd(Cp)(η^3-C_3H_5)	4c	2.48	3.3 ± 0.5	Pd	172
Pd(η^3-C_3H_5)(Cp)	4d	4.04	4.0 ± 0.5	Pd	159
$Pt(hfa)_2$	5a	1.70 −5.70	10−100	Pt, C	
$PtMe_2$(cod)	5b	1.02	<1	Pt	172
$PtMe_2$(cod)	5c	2.30	3.0 ± 0.5	Pt	170
$PtMe_2$(cod)	5d	3.80	2.7 ± 0.5	Pt	175

sure is expected to be reduced or absent. In the present case, the conditions we have chosen, a flow of hydrogen less than 10% of that of the helium carrier gas introduced immediately before the planar support or the fluidized bed, combined with the adequate thermal stability of the precursors allow to minimize reactions in the gas phase. Increasing the temperature or the concentration of hydrogen leads indeed to gas-phase decomposition, as indicated by the formation of metallic dust during the experiments. However, in the concentration ranges we used, hydrogen significantly decreases the temperature of decomposition while pure and adherent deposits are formed. The great reactivity of the complexes toward hydrogen (except for $Pt(hfa)_2$) is reflected in the rapid deposition of the metal and thus the decomposition step is expected to be easy and rapid. Consequently, the adsorption phenomenon represents probably the critical step in our conditions.

The ratio surface of substrate/volume of gas differs markedly from one substrate to the other one: 1−45 from planar to divided supports. The porous silica offers a dramatically higher number of anchoring sites where crystallites can grow. The hydrodynamics of the two processes are different with a bubbling regime in the fluidized bed and a laminar regime on planar supports. These differences can partially explain the crystallites dispersion as small aggregates of nanometric size. In the fluidized bed, the homogeneity is largely favored by the hydrodynamic of the process. Indeed, the bubbling regime allows a great contact of all the surface of the support with the gas phase and can be easily assimilated to a good mixing of the reactants in a liquid phase. Even if the precursor is fully transformed in the first part of the bed, this hydrodynamic regime certainly favors the nucleation step with regard to the growth step. In addition, the low temperatures used for the deposition prevent the migration and coalescence of the aggregates on the silica surface.

The use of an on-line mass spectrometer has demonstrated that the organic products of the decomposition of the precursor on deposition on a divided support are identical to those observed on deposition on a planar support (Table 5). The presence of hydrogen allows the organic ligands to be cleanly eliminated as stable, volatile organic molecules, hence minimizing the cleavage of internal ligand bonds. It is worth to mention that this general mechanism is supported, *a contrario* by the behavior of $Pt(hfa)_2$. A part of the complex is adsorbed on the solid in a first step. The decomposition through metal−ligand bond breaking is slow and disfavored with regard to internal breaking of bonds of the ligands, providing nonvolatile carbon-containing compounds which can explain the heavy contamination of the deposit on both planar and divided supports. Finally, the decomposition yield is reduced roughly to 25% in both cases. Although the powders contain a great number of sites, large amounts of $Pt(hfa)_2$ pass through the fluidized bed, regardless of the experimental conditions we have examined.

It is commonly assumed that the steps that generate the divided catalytic species in traditional elaboration of catalysts are the crucial ones (for instance calcination in the classic impregnation method).[1,19a,20] Similar deciding steps, driven by the competing effect of nucleation and growth have evidently also a great influence on our chemical vapor deposition method. Thus, it seems of interest to identify the fundamental parameter linked to both nucleation rate and growth rate.[19]

From the works of Marcilly,[19a] the homogeneous nucleation rate in a fluid matrix (N_r) can be simply expressed as

$$N_r = n_c S_c F_r \tag{1}$$

where n_c is the number of critical germs (stable particles with minimal size) by volume unit, S_c is the surface of the critical germ, and F_r is the rate of fixation of the dissolved monomer entities by surface unit ot the germs. From eq 1, N_r can be expressed as a function of the supersaturation ratio (S):[21]

$$N_r = S_c F_r n \exp(A/k^3T^3 \log^2 S) \tag{2}$$

S is defined as the ratio C/C_∞ where C is the concentration of gaseous species near the growing surface and C_∞ is the concentration of gaseous species near an infinite planar surface of the solid formed. Equation 2 demonstrates the exponential variation of the homogeneous nucleation rate with an increasing supersaturation ratio. On the heterogeneous nucleation rate, the supersaturation ratio influence is greater due to the presence of solid defaults, which assist the nucleation of the particles. The Strickland−Contable model gives,[22] as for it, the growth rate (G_r) as a linear function of the supersaturation ratio:

$$G_r = BC_\infty(S - 1)^{21} \tag{3}$$

The examination of eqs 2 and 3 clearly shows that a high supersaturation ratio greatly favors the nucleation rate in comparison with the growth rate, and so should

(19) (a) Marcilly, C. In *Fundamental and Industrial Aspects of Catalysis by Metals*; Imelik, B., Martin, G.-A., Renouprez A.-J., Eds; CNRS: Paris, 1984; p 121. (b) Zettlemoyer, A. C. *Nucleation*; Dekker: New York, 1969. (c) Walton A. G. *The Formation and Properties of Precipitates*; Intersciences Publishers (div. of John Wiley and Sons): London, 1967.

(20) Anderson, J. R. *Structure of Metallic Catalysts*; Academic Press: London, 1975.

(21) Note: n_c from eq 1 can be expressed by a Boltzmann law: $n_c = n \exp(-\Delta\mu_c/kT)$ where n is the number of monomer entities by volume unit, $\Delta\mu_c$ is the enthalpy of critical germ formation, k is the Boltzmann constant and T the temperature. $\Delta\mu_c$ can be expressed as a function of the supersaturation ratio $S = C/C_\infty$: $-\Delta\mu_c = A/(k^2T^2 \log^2 S)$, where A is a constant including the volume of a critical germ and the interfacial enthalpy by surface unit. Equation 2 is obtained from the two previous expressions injected in eq 1. In eq 3 B is a constant depending on the type of the growth (dislocation, spiral, etc.).

(22) Strickland-Contable, R. F. *Kinetics and Mechanism of Crystallisation*; Academic Press: London, 1968.

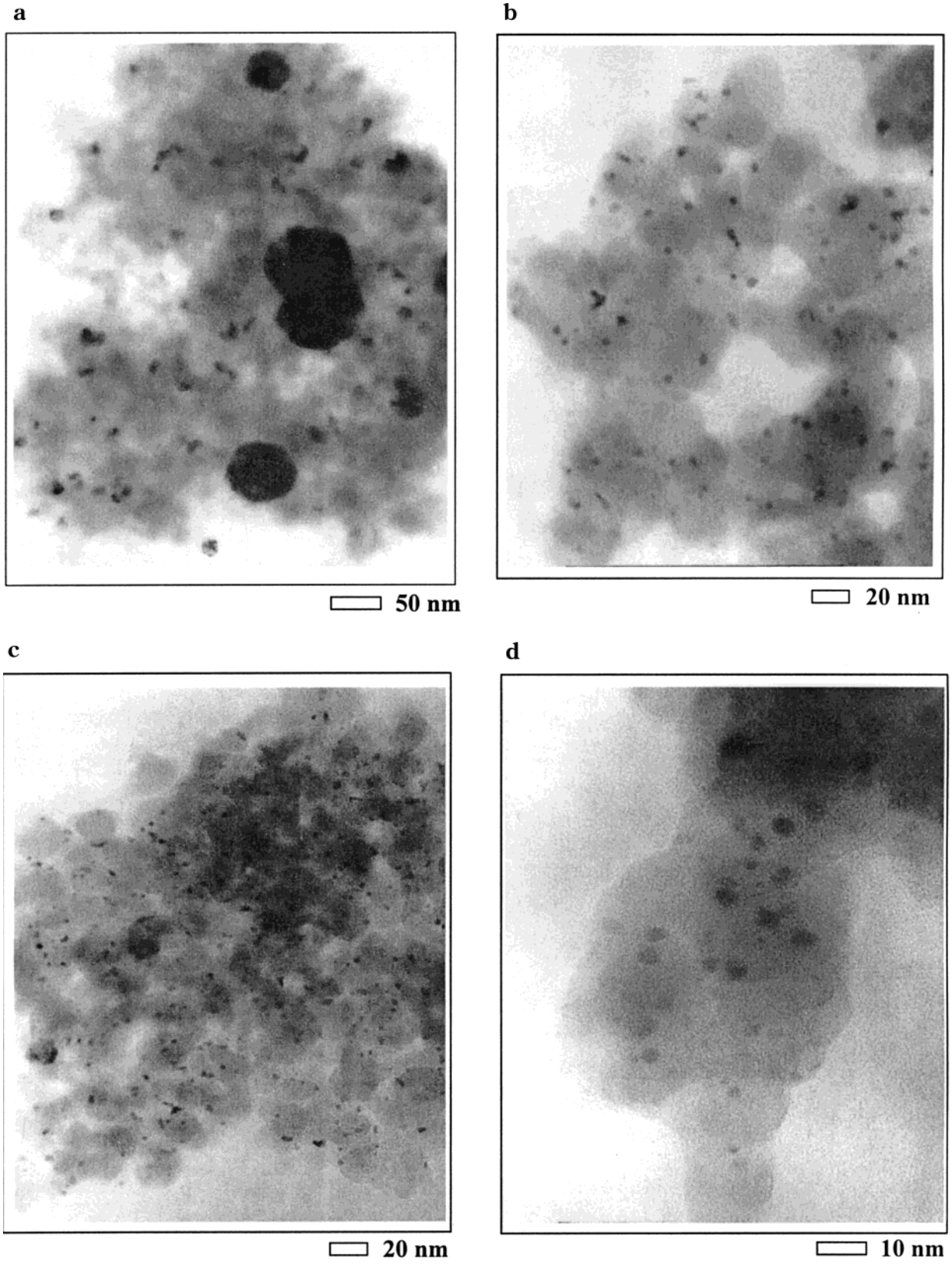

Figure 5. Transmission electron microscopy (TEM) photographs of platinum deposits supported on silica: (a) $Pt(hfa)_2$, (b) Pt/SiO_2 2.30 wt %, (c) overview of Pt/SiO_2 3.80 wt %, and (d) enlargment Pt/SiO_2 3.80 wt %.

permit a wide number of small particles to be obtained instead of large crystallites much less dispersed.

To clarify the supersaturation role in our process, experiments were carried out at different sublimation temperatures. The temperature dependence of the vapor pressure for the platinum complexes have shown that the higher concentrations in gaseous species (and so the higher supersaturation ratios) are obtained for the higher temperatures. Platinum deposits on silica from $PtMe_2(cod)$ were carried out at sublimation temperatures of 29 and 95 °C, all other parameters being equal. The results are displayed on Table 6. Obviously, the

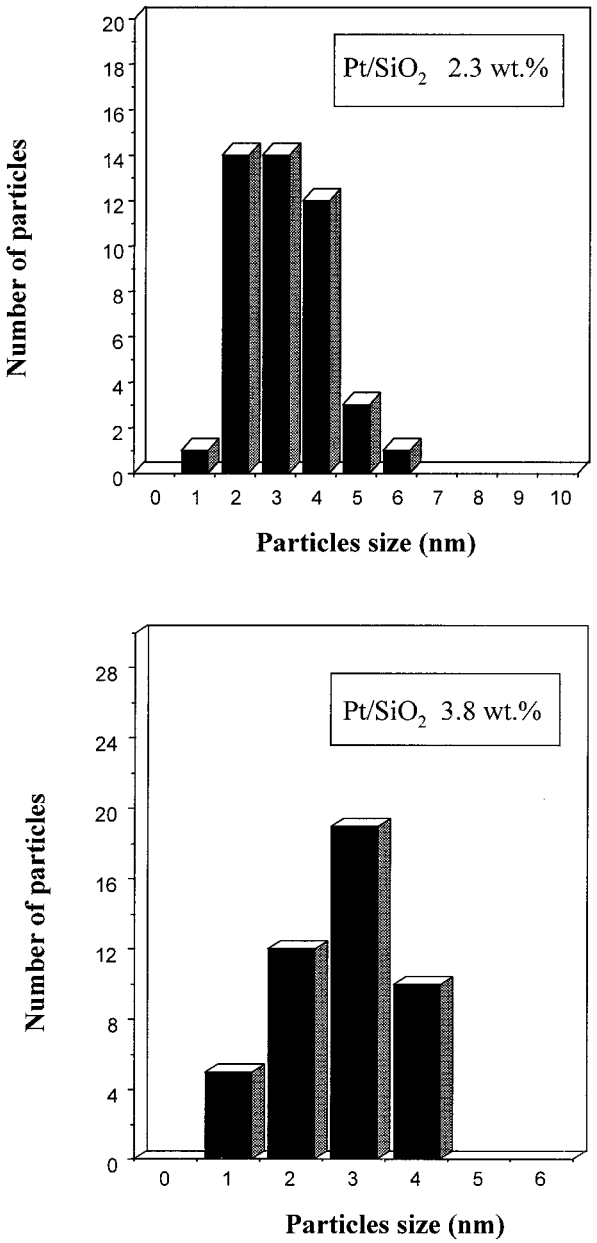

Figure 6. Histograms of the particles size for platinum deposits from $PtMe_2$(cod).

Table 5. Identification by On-Line Mass Spectrometry of the Organic Residues from MOCVD Experiments

precursors	decomposition products
Pd(Cp)(η^3-C_3H_5)	propane, propene, cyclopentane, cyclopentene, cyclopentadiene
Pd(η^3-C_3H_5)(hfa)	propane, propene, trifluoropropanone, various organofluoride products
$PtMe_2$(cod)	pethane, cyclooctane, cyclooctene, cyclooctadiene

Table 6. FBMOCVD Experiments from $PtMe_2$(cod) Sublimated at 29 and 95 °C

	sublimation T (°C)	deposition T (°C)	vapor P (mTorr)	av particle size (nm)
run 1	29	110	3.7	50−70
run 2	95	110	93.3	2−6

molar ratio precursor/carrier gas is highly supersaturated in the first experiment compared to the second, and so leads to the formation of numerous nanoparticles (Figure 5b). In the opposite, in the case of the second experiment, large crystallites of a size greater than 50 nm are obtained (Figure 7). These observations are consistent with the results and equations previously stated, and provide the first indication that can confirm the role of the supersaturation ratio to prepare small and dispersed aggregates by CVD in a fluidized bed. The general importance of the supersaturation ratio of the medium in the field of catalysts preparation was already underlined by the work of Roginskij as early as 1936;[23] however, this parameter is very often ignored in the literature concerning the preparation of the catalysts.

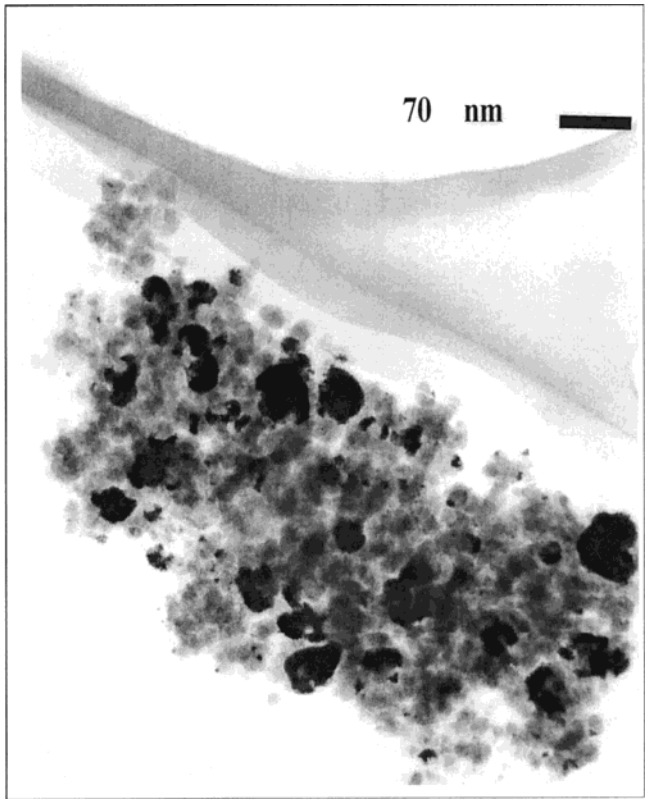

Figure 7. TEM photograph of Pt/SiO_2 3 wt % obtained from $PtMe_2$(cod) at 29 °C.

Thus, when high supersaturation conditions and high conversion rates due to favorable chemical conditions can be reached, it is readily easy to promote the formation of very small particles of pure metal, homogeneously and well-dispersed on a porous support having a great specific area.

Finally the catalysts prepared by FB-MOCVD of palladium and platinum on porous silica were highly active for the dehydrogenation of cyclohexane.[24] It is worth noting that the activity of the catalysts was completely stable over repeated runs. Microscopic examination did not reveal any change in the size or the

(23) Roginskij, S. Z. *Acta Physicochim.***1936**, *4*, 729.

(24) Note: The results of conversion and turnover are the following: Pd 0.7 wt %, 100% benzene, 1835 h^{-1}; Pd 2.48 wt %, 100% benzene, 730 h^{-1} ; Pt 0.35 wt %, 40% benzene, 60% cyclohexene , 1020 h^{-1} ; Pt 0.7 wt %, 95% benzene, 5% cyclohexene, 1300 h^{-1}. The turnover numbers given are relative to the total mass of metal present on the silica, and take no account of the slightly different aggregate sizes in the different catalysts. Even at relatively low conversion levels, the palladium catalysts are completely specific for the formation of benzene, and no cyclohexene was observed. However, cyclohexene was observed when the reaction was catalyzed with platinum, and was the majority product when the reaction was carried out under a regime of low conversion.

distribution of the aggregates.[25] Hence the nanoparticles produced by FB-MOCVD are stable toward migration (sintering) and agglomeration even at temperatures largely higher than those used for their preparation.

Conclusion

Two platinum complexes, $Pt(hfa)_2$ and $PtMe_2(cod)$ as well as two palladium complexes, $Pd(Cp)(\eta^3\text{-}C_3H_5)$ and $Pd(\eta^3\text{-}C_3H_5)(hfa)$, have been selected to produce by MOCVD platinum and palladium deposits on planar and on divided supports. Using the CVD method in a fluidized bed under reduced pressure conditions has allowed the deposition of the metals on porous divided substrates. Introduction of hydrogen in the carrier gas not only results in a dramatic decrease of the decomposition temperature, due to an easier loss of the ligands, but also provides more pure deposits. The study on planar substrates has shown that $PtMe_2(cod)$, $Pd(Cp)(\eta^3\text{-}C_3H_5)$, and $Pd(\eta^3\text{-}C_3H_5)(hfa)$ are suitable precursors to produce pure deposits under remarkably low temperatures. In contrast, $Pt(hfa)_2$ gave poor results since the deposits are contaminated with fluorine, oxygen, and principally carbon. Under the reduced pressure that we used to combine the vaporization of the complexes and a bubbling regime for the fluidized bed, the partial pressure of the metal complexes can be maintained at a relatively high level. Thus, for the preparation of a catalyst with highly dispersed metallic particles, a high supersaturation regime was shown to be a crucial parameter, allowing a good nucleation rate with regard to the growth rate to be favored.

The present study has shown that for a given precursor, the conditions determined for the deposition of a metal on a planar support can be transposed to those required for the preparation of a catalyst. The thorough study of thin films MOCVD gives decisive information for preparing supported catalysts.

Experimental Section

$Pd(Cp)(\eta^3\text{-}C_3H_5)$, $Pt(hfa)_2$, and $PtMe_2(cod)$ were prepared according to literature methods.[26−28] ^{1}H NMR spectra were recorded on a Brüker AC200 spectrometer. Electron impact mass spectra were recorded at 70 eV on a NERMAG R10-10 spectrometer. TGA/DTC experiments were conducted on a B60 DAM Sétaram apparatus.

(η^3-Allyl)(hexafluoroacetylacetonato)palladium. This compound was prepared by a modification of the method reported by Yuan and Puddephatt.[29]

Palladium dichloride (4.2 g, 23.7 mmol) was dissolved in 20 mL of aqueous sodium chloride solution (2.7 g, 45.1 mmol NaCl) at 40 °C. The resulting solution of sodium tetrachloropalladate was diluted with 100 mL of methanol, and 6.4 mL (78 mmol) of allyl chloride was added dropwise. The mixture was refluxed for 45 min while carbon monoxide was bubbled through it. After the solution was cooled to room temperature, it was extracted with chloroform (4 × 30 mL), and the organic extract was dried and evaporated to yield 4.15 g bis(η^3-allyl)-dichlorodipalladium (95% yield) as a yellow powder.

A solution of 0.64 g (16 mmol) of sodium hydroxide and 3.1 g (14.9 mmol) of hexafluoroacetylacetone in 70 mL of water was added dropwise to a suspension of 2.0 g (5.5 mmol) of $[PdCl(\eta^3\text{-}C_3H_5)]_2$ in 400 mL of diethyl ether. The mixture was stirred vigorously for 10 min. The organic layer was separated, dried, and evaporated. The crude product was purified by sublimation at 30−40 °C under 0.1 Torr to yield 2.1 g of (η^3-allyl)(hexafluoroacetylacetonato)palladium (90%) as yellow crystals. ^{1}H NMR (200.13 MHz, $CDCl_3$): $\delta = 3.15$ (d, $^2J_{HH} = 7$ Hz, 2H), 4.21 (d, $^2J_{HH} = 12$ Hz, 2H), 5.72 (tt, $^2J_{HH} = 7$ Hz, 12 Hz, 2H), 6.1 (s, 1H). IR (KBr disk): $\nu(CO) = 1672$ cm^{-1}. MS (peaks for the ^{106}Pd isotopomer): $m/q = 354$ (40%), 285 (10%), 147 (100%), 106 (30%), 69 (52%), 41 (27%), 39 (85%).

CVD on Planar Supports. CVD on planar supports was carried out in a classical hot wall reactor of 11 mm internal diameter described elsewhere.[12] The carrier gas was helium at ∼50 Torr. When used, hydrogen was introduced into the carrier gas stream immediately before it reached the substrate, to minimize gas-phase reactions.

FB-MOCVD on Silica Powder. The fluidized bed reactor was previously described.[5] The silica powder is supported on a stainless steel mesh of 25 μm opening. The precursor complex is supported on a sintered glass frit of porosity 5.

In a typical experiment, 0.4 g of $PtMe_2(cod)$ was introduced into the lower part of the reactor and 4 g of silica powder (sieved between 100 and 200 μm) were introduced into the upper part. The reactor was evacuated to 0.1 Torr and kept at this pressure for 1 h while the silica powder was heated to 100 °C by ethylene glycol passing through a double envelope in the reactor wall. After this time, the silica powder was heated to 110 °C (the deposition temperature) and the pressure inside the reactor was raised to 30 Torr by the addition of helium (helium flow: 86 mL mn^{-1}) at the bottom of the reactor. This pressure was determined so that the velocity of gas through the fluidized bed was approximately four times the minimum bubbling velocity of the powder. The lower portion of the reactor was then heated to 80 °C to sublime the complex into the stream of helium, and a stream of hydrogen was introduced just before the fluidized bed. After 2.5 h, the heating was stopped and the reactor allowed to cool to room temperature. The pressure was returned to atmospheric pressure, and the silica powder was recovered. Deposition conditions are given in Table 3.

Dehydrogenation of Cyclohexane. A total of 1.0 g of catalyst was supported in a borosilicate glass tube of 15 mm internal diameter by loose plugs of glass wool. This was connected to an evaporator containing 100 g of cyclohexane at a temperature of 90−100 °C. The catalyst bed was heated by a tube furnace to 300−500 °C. A stream of helium carried the cyclohexane from the evaporator into the reaction tube, and then the products of the reaction into a liquid nitrogen cold trap. The duration of the experiment was the time taken for all the cyclohexane to be evaporated: this was adjusted by varying the temperature of the evaporator and the flow of helium carrier gas. The yields of products were determined by gas chromatography (Econo-Cap FFAP column, Alltech Associates, Deerfield, IL) with anisole as an external standard.

Acknowledgment. The authors thank Engelhard-CLAL for their generous loan of palladium and platinum salts. The authors also thank E. Azeau and are grateful to Dr. Nigel Wheatley for his assistance.

Supporting Information Available: Two figures showing the thermal analysis of $Pt(hfa)_2$ and the vapor pressure vs temperature curves of $Pt(hfa)_2$ and $PtMe_2(cod)$. This material is available free of charge via the Internet at http://pubs.acs.org.

CM990406E

(25) Unpublished results.
(26) $Pd(Cp)(\eta^3\text{-}C_3H_5)$: Shaw, B. L. *Proc. Chem. Soc.* **1960**, 247.
(27) $Pt(hfa)_2$: Okeya, S.; Kawaguchi, S. *Inorg. Synth.* **1980**, *20*, 65.
(28) $PtMe_2(cod)$: Clarck, H. C.; Manzer, L. E. *J. Organomet. Chem.* **1973**, *59*, 411.
(29) Yuan, Z.; Puddephatt, R. J. *Adv. Mater.* **1994**, *1*, 6.